An improved study of HCO⁺ and He system: Interaction potential, collisional relaxation, and pressure broadening ⊘

F. Tonolo [iD] ; L. Bizzocchi ✉ [iD] ; M. Melosso [iD] ; F. Lique ✉ [iD] ; L. Dore [iD] ; V. Barone [iD] ; C. Puzzarini ✉ [iD]

Check for updates

CrossMark

View Online

Export Citation

24 January 2024 14:39:16

An improved study of HCO⁺ and He system: Interaction potential, collisional relaxation, and pressure broadening

View Online   Export Citation   CrossMark

F. Tonolo,[1,2] [iD] L. Bizzocchi,[1,2,a] [iD] M. Melosso,[2] [iD] F. Lique,[3,a] [iD] L. Dore,[2] [iD] V. Barone,[1] [iD] and C. Puzzarini[2,a] [iD]

AFFILIATIONS

[1] Scuola Normale Superiore, Piazza dei Cavalieri 7, I-56126 Pisa, Italy
[2] Dipartimento di Chimica "Giacomo Ciamician", Università di Bologna, Via F. Selmi 2, I-40126 Bologna, Italy
[3] Univ. Rennes, CNRS, IPR (Institut de Physique de Rennes)–UMR 6251, F-35000 Rennes, France

[a] Authors to whom correspondence should be addressed: luca.bizzocchi@unibo.it; francois.lique@univ-rennes1.fr;
and cristina.puzzarini@unibo.it

ABSTRACT

In light of its ubiquitous presence in the interstellar gas, the chemistry and reactivity of the HCO⁺ ion requires special attention. The availability of up-to-date collisional data between this ion and the most abundant perturbing species in the interstellar medium is a critical resource in order to derive reliable values of its molecular abundance from astronomical observations. This work intends to provide improved scattering parameters for the HCO⁺ and He collisional system. We have tested the accuracy of explicitly correlated coupled-cluster methods for mapping the short- and long-range multi-dimensional potential energy surface of atom–ion systems. A validation of the methodology employed for the calculation of the potential well has been obtained from the comparison with experimentally derived bound-state spectroscopic parameters. Finally, by solving the close-coupling scattering equations, we have derived the pressure broadening and shift coefficients for the first six rotational transitions of HCO⁺ as well as inelastic state-to-state transition rates up to $j = 5$ in the 5–100 K temperature interval.

Published under an exclusive license by AIP Publishing. https://doi.org/10.1063/5.0075929

I. INTRODUCTION

The harsh conditions of the interstellar medium (ISM) pose severe constraints to the chemical processes it hosts, which exhibit behaviors that greatly differ from those occurring in terrestrial environments. For instance, in space, the molecular energy level populations are rarely at local thermodynamic equilibrium (LTE) since the density is usually so low ($\sim 10^2$–10^6 cm^{-3}) that collisions compete with radiative processes. Under such conditions, the estimate of molecular abundances in the ISM from spectral lines requires the knowledge of their collisional coefficients for the most abundant perturbing species. Their nature depends on the investigated interstellar environment, being for most cases neutral species such as H₂ or He,[1] but also collisions with electrons should be considered in photon dominated regions.[2] In this context, the study and computation of the collisional parameters has gained an increasing interest, the aim being the balance between accuracy and computational cost.

In this work, we benchmarked the performance of different levels of theory in describing the interaction potential of a collisional system. With the aim of extending the discussion also to larger systems, we kept a keen eye on the computational cost. A remarkable outcome in this regard exploits the good performances of explicitly correlated coupled-cluster methods[3–8] for mapping the short- and long-range multi-dimensional potential energy surface (PES) of collisional systems.

The system we opted to investigate addresses the collision between the HCO⁺ ion with He. As far as we know, this study reports the first application of explicitly correlated methods to this collisional system and represents the most accurate description of the underlying interaction potential, while maintaining an affordable computational cost. Moreover, given the great relevance of ion chemistry in terms of the molecular evolution of the interstellar medium, the HCO⁺ ion is particularly interesting:[9] it is the most abundant cation in dense molecular clouds[10] and has been detected in a large number of objects with widely differing physical

characteristics[11–13] (see also Ref. [14] for an exhaustive list of recent detections). For this reason, it has a prominent role when seeking for new interstellar chemical networks and has been often used as a tracer of ionization in different dense interstellar cores.[15]

The first interstellar detection of the HCO^+ ion dates back to 1970,[16] albeit its identification was not unambiguously verified until the characterization of its rotational spectrum in 1975.[17] Given its astrochemical relevance, several previous studies have determined the experimental and computational counterparts for some of the HCO^+ scattering parameters. The first set of rotational de-excitation rate coefficients of HCO^+ in collision with both *para*− and *ortho*−H_2 was recently determined by Denis-Alpizar et al.[18] As regards the HCO^+ and He collisional system, the computation of the first state-to-state rate coefficients dates back to 1985.[19] Afterward, in 2008, Buffa et al.[20] characterized a new PES by employing the CCSD(T) method (coupled cluster singles, doubles, with a perturbative treatment of triples excitations)[21] in conjunction with a quadruple-ζ quality basis set (aug-cc-pVQZ),[22] from which the pressure broadening and pressure shift parameters were then derived.[20] In the same work, the experimental results obtained by means of a frequency modulated spectrometer for three rotational lines of HCO^+ at 88 K have been reported. Shortly after, starting from the same PES, the corresponding state-to-state rates have also been computed.[23] Finally, in 2019, Salomon *et al.* experimentally determined, employing the double resonance technique, the rotational parameters associated with the ground state of the bound system He–HCO^+.[24] The comparative analysis of such data with those obtained in this work has therefore permitted a robust validation of the employed methodologies.

This paper is organized as follows. Section II provides an in-depth analysis leading to the choice of the level of theory for the description of the PES of the collisional system. Section III shows the subsequent derivation of the rotational parameters of the bound state, which led to a further validation of the computed potential by comparison with the experimental results. Finally, Sec. IV describes the performed quantum scattering computations and the derived parameters: the computation of the inelastic cross section is detailed in Sec. IV A, while the inelastic rate coefficients between the rotational states of the system and the pressure broadening and pressure shift coefficients are presented in Secs. IV B and IV C, respectively.

II. CONSTRUCTION AND TESTING OF THE POTENTIAL ENERGY SURFACE

The starting point of our study on the HCO^+ and He collisional system is the accurate investigation of its intermolecular PES. We describe the system using standard Jacobi coordinates, i.e., the distance between the center of mass of HCO^+ and the He atom (R) and the angle θ between the molecular axis and R distance vector (see Fig. 1).
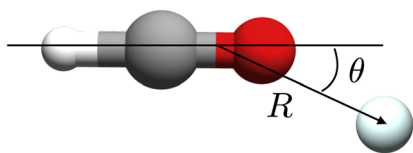

FIG. 1. Jacobi internal coordinates of the HCO^+ and He collisional system.

The lowest vibrational mode of the HCO^+ ion lies at ~829 cm^{-1} (see Ref. [25]). Therefore, under the non-reactive low-temperature conditions, which we target in the present investigation, all the vibrational channels can be safely considered as closed. Accordingly, the HCO^+ structure was held fixed to its experimentally determined r_e geometry,[26] linear and with C–H and C–O bond distances of 1.0920 and 1.1056 Å, respectively.

For the *ab initio* calculation of the interaction energy, the choice of the level of theory that best combines accuracy and computational efficiency was guided by a preliminary benchmark study on a sample of 25 geometries that tested different methodologies and basis sets. The results are reported in Table I.

Given the strong ionic effect of HCO^+, a sufficiently flexible basis set is needed to describe the electronic behavior in regions far from the electronic density maximum. For this reason, two triple-ζ correlation-consistent basis sets,[27] which introduce diffuse functions in a complete (aug-) or partial (jun-) way, have been evaluated.[6,28,29] As shown for many molecular systems involving non-covalent interactions, the partial addition of diffuse functions accurately predicts the electronic behavior while saving computational cost.[30] The chosen basis sets are the aug-/jun-cc-pVnZ and the method employed for all computations is CCSD(T).[31] In addition, a bi-electronic distance dependence in the Slater-type form can be included in the electronic wave function. This contribution enhances the performance of the wavefunction for small interelectronic separations and has been demonstrated in many cases to be very suitable for mapping the short- and long-range multi-dimensional PESs.[7,8] The methods that introduce this contribution are the so-called explicitly correlated methods with the F12 approximation being employed.[3–5] In detail, the CCSD(T)-F12a method has been used in combination with both the jun-/aug-cc-pVTZ basis sets and within the frozen core approximation (fc). All calculations were carried out with the MOLPRO program suite.[32]

Going into the details of the test, the CCSD(T)-F12 energies were compared with those obtained via the CCSD(T)/CBS (complete basis set) composite scheme in which extrapolation to the CBS limit has been achieved according to two different procedures, having different computational costs. In the first approach, the total energy is defined as

$$E_{tot} = E_{HF}^{\infty} + \Delta E_{CCSD(T)}^{\infty}. \tag{1}$$

Here, the first term on the right-hand side is the HF-SCF energy, extrapolated to the CBS limit by means of Feller's exponential formula[33]

$$E_{HF}^{\infty} = E_{HF}^n - B\,e^{-Cn}, \quad n = 3, 4, 5. \tag{2}$$

The second term of Eq. (1) accounts for the extrapolation to the CBS limit of the CCSD(T) correlation energy (E_{corr}) within the fc approximation, using the two-point n^{-3} formula by Helgaker *et al.*,[34]

$$\Delta E_{CCSD(T)}^{\infty} = \frac{n^3 E_{corr}^n - (n-1)^3 E_{corr}^{n-1}}{n^3 - (n-1)^3}, \tag{3}$$

where $n = 4$.

Alternatively, the total energy is obtained by applying the mixed Gaussian-exponential formula by Peterson *et al.*[22]

$$E_n = E_{CBS} + \alpha e^{-(n-1)} + \beta e^{-(n-1)^2}, \tag{4}$$

TABLE I. CP-corrected interaction energies (cm^{-1}) for different geometries of the HCO^+ and He collisional system.

Geometry		Peterson CBS extrapolation[a]		Feller + Helgaker CBS extrapolation[b]			CCSD(T)-F12[a]	
R	θ	aug-cc-pVnZ	jun-cc-pVnZ	aug-cc-pVnZ	jun-cc-pVnZ	aug-cc-pVQZ	aug-cc-pVTZ	jun-cc-pVTZ
2.0	0.0	16 670.07	16 674.57	17 812.85	17 689.38	16 763.42	16 717.49	16 752.53
3.5	0.0	−66.41	−61.07	−8.77	−24.23	−61.02	−69.90	−60.37
5.0	0.0	−15.40	−16.70	−8.41	−8.83	−15.66	−15.64	−14.17
7.5	0.0	−0.90	−2.20	−0.73	−0.68	−2.91	−2.90	−2.36
10.0	0.0	1.30	−0.01	0.80	0.82	−0.93	−0.97	−0.78
2.0	45.0	6 313.38	6 315.28	7 348.92	7 220.16	6 370.79	6 340.73	6 379.80
3.5	45.0	−70.39	−66.35	−26.91	−39.02	−69.54	−71.53	−61.78
5.0	45.0	−14.09	−16.70	−9.72	−10.01	−16.13	−16.03	−14.10
7.5	45.0	−0.90	−2.20	−0.96	−0.84	−3.08	−3.11	−2.52
10.0	45.0	1.30	−0.01	0.74	0.70	−0.99	−1.04	−0.83
2.0	90.0	2 139.73	2 139.50	2 741.54	2 634.35	2 177.23	2 152.64	2 196.11
3.5	90.0	−91.50	−85.25	−59.17	−66.54	−89.72	−91.22	−81.39
5.0	90.0	−18.49	−18.90	−15.30	−14.50	−20.46	−20.26	−18.10
7.5	90.0	−4.40	−5.70	−1.87	−1.52	−3.84	−3.82	−3.19
10.0	90.0	1.30	−2.20	0.57	0.52	−1.19	−1.23	−1.00
2.0	135.0	9 549.84	9 543.82	10 301.07	10 195.37	9 623.74	9 578.38	9 620.42
3.5	135.0	−178.60	−171.79	−123.26	−138.63	−171.77	−174.03	−158.42
5.0	135.0	−33.90	−32.09	−29.97	−28.07	−35.98	−35.93	−32.66
7.5	135.0	−3.10	−4.40	−3.60	−3.02	−5.52	−5.48	−4.72
10.0	135.0	−2.20	−2.20	0.16	0.25	−1.55	−1.58	−1.31
2.0	180.0	191 024.32	191 019.68	193 450.01	193 365.57	191 419.52	191 286.67	191 318.90
3.5	180.0	−269.65	−271.98	−126.56	−155.74	−265.64	−268.54	−250.38
5.0	180.0	−60.70	−50.55	−49.50	−48.73	−58.24	−58.93	−53.99
7.5	180.0	−5.29	−7.90	−5.01	−4.28	−6.97	−6.84	−6.03
10.0	180.0	−2.20	−2.20	−0.17	0.00	−1.80	−1.80	−1.53
CPU time[c]		9 000	7 400	8 500	4 300	8 500	2600	1700

[a]Extrapolation to the CBS limit of the fc-CCSD(T) energies performed with the Peterson three-point extrapolation formula with $n = 3, 4, 5$.
[b]The extrapolation of the HF-SCF energy performed with the three-point formula by Feller ($n = 3, 4, 5$), combined with the extrapolation of the fc-CCSD(T) correlation energy using the two-point ($n = 3, 4$) formula by Helgaker.
[c]Mean CPU time (s) needed to compute one point of the energy grid (rounded values).

where E_{CBS}, α, and β are adjustable parameters and $n = 3, 4, 5$. The energies derived via this extrapolation on fully augmented basis sets were taken as reference energies in the benchmark test.

The interaction energy E_{int} has been determined as follows:

$$E_{int} = E_{AB} - (E_A + E_B), \quad (5)$$

where E_{AB} is the molecular complex energy, while E_A and E_B are the energies of the two fragments. The interaction energies have also been corrected by a counterpoise (CP) contribution in order to balance out the energy overestimation given by the basis set superposition error (BSSE). The CP correction is computed using the Boys and Bernardi formula[35]

$$\Delta E_{CP} = \left(E_A^{AB} - E_A^A \right) + \left(E_B^{AB} - E_B^B \right), \quad (6)$$

where E_X^{AB} is the energy of the monomer calculated with the same basis functions used for the cluster and E_X^X is the energy of the monomer computed with its own basis set (X = A, B).

Inspection of Table I illustrates the remarkably good performances of the F12-explicitly correlated methods, which provide a description of long- and short-range energy interactions in good agreement with that obtained via the computationally expensive Peterson CCSD(T)/CBS extrapolation scheme ($n = 3, 4, 5$). Going into detail, the short-range energy comparison reveals a mean percentage error around 5%. At long range, the low value of the energies makes the percentage error comparatively higher. However, the difference between the energies is always lower than 2.5 cm^{-1}. On the other hand, the cheaper Feller and Helgaker composite scheme, which exploits smaller basis sets ($n = 3, 4$) for the extrapolation of the CCSD(T) correlation energy, fails to predict the energy trend with the same accuracy. Table I also shows that the F12 method in combination with a triple-ζ quality basis set performs slightly better than the conventional CCSD(T) model in conjuction with the aug-cc-pVQZ basis set. To date, the latter level of theory provides the most accurate PES available in the literature for the collisional system of interest.[20]

A further remarkable feature is that the use of partially augmented (jun-) basis sets does not significantly affect the description of the PES except, as expected, in the long-range regions, where the dispersive interactions provide a major contribution to the energy. Given the lower computational cost entailed, however, the jun-cc-pVTZ basis set may be still recommended for systems whose long-range interactions are less prominent.

On the basis of this benchmark test, in the present work, the PES of the HCO^+ and He collisional system has been entirely investigated by employing the CCSD(T)-F12a/aug-cc-pVTZ model, which is the level of theory that offers the best compromise between accuracy and computational cost. The interaction potential has been built from an irregular grid in the R, θ coordinates. A total of 390 points have been chosen by sampling the portion of the PES for R varying between 2 and 10 Å and for 13 θ values equally spaced throughout the molecular plane. The radial mesh is denser in the region between 2 and 4 Å in order to sample the energy behavior in the proximity of the potential well, where sizable anisotropic effects are expected. Since we are dealing with a new potential energy surface for the system under investigation, a .tar archive containing the computed interaction energies for each set of Jacobi coordinates (R, θ) has been incorporated in the supplementary material.

For the solution of the nuclear Schrödinger equation by means of the close coupling equations, it is useful to express the interaction potential as an expansion of angular functions. For an interaction system formed by a linear rigid rotor and an atom, we can define the potential as

$$V(R, \theta) = \sum_{\lambda} v_{\lambda}(R) P_{\lambda}(\cos \theta), \quad (7)$$

where $P_{\lambda}(\cos \theta)$ is a Legendre polynomial and $v_{\lambda}(R)$ are the radial coefficients.[36] The polynomial expansion has been performed on 13 points ($\lambda_{max} = 12$), i.e., on the number of θ angles at which the PES is sampled. Different λ terms ($\lambda > 0$) govern the magnitudes of the inelastic rotational transitions, allowing for changes of the molecular angular momentum by $\Delta j = \pm \lambda$. Likewise in all the molecular ion–atom collisions, the long-range parts of the potential are characterized by a sizable contribution due to the induction interactions. This contribution scales with the interparticle distance as R^{-4} and is proportional to the square of the charge of HCO^+ and to the static electric dipole polarizability of helium. To ensure a correct behavior of the PES expansion at large distances, the radial coefficients $v_{\lambda}(R)$ have been fitted to the functional form,

$$v_{\lambda}(R) = e^{-a_1^{\lambda}R}\left(a_2^{\lambda} + a_3^{\lambda}R + a_4^{\lambda}R^2 + a_5^{\lambda}R^3\right)$$
$$- \frac{1}{2}\left[1 + \tanh R/R_{ref}\right]\left(\frac{C_4^{\lambda}}{R^4} + \frac{C_6^{\lambda}}{R^6} + \frac{C_8^{\lambda}}{R^8} + \frac{C_{10}^{\lambda}}{R^{10}}\right), \quad (8)$$

where the C_n^{λ} symbols are used to label the coefficients of the R^{-n} terms. The hyperbolic tangent factor provides a smooth transition between the short-range region ($0 < R < R_{ref}$), where computed PES points are available, and the long-range extrapolated domain ($R > R_{ref}$). The analytic potential was found to accurately reproduce the calculated energies. The difference between the *ab initio* points and the values obtained from Eq. (8) and the fitted radial coefficients is less than 1% across the entire grid. A contour plot of the potential derived from the fit is shown in Fig. 2. The potential shows a global minimum when helium is collinear with the collider and interacts
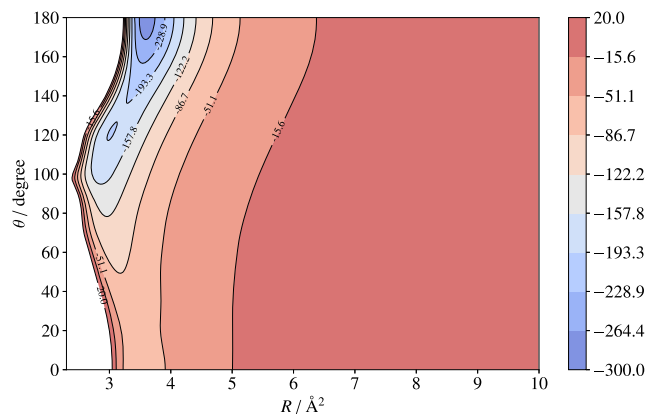

FIG. 2. Contour plot of the HCO^+ and He interaction PES as a function of R and θ. Energies are in cm^{-1}.

with the hydrogen of HCO^+ at $R = 3.6$ Å. The resulting interaction energy in this point is 279.78 cm^{-1}.

III. BOUND STATES

A way for validating the new computed PES of the collisional system is provided by the calculation of the bound-state energies, whose experimental values are available.[24] For this purpose, the BOUND program has been employed.[37] The reduced mass of the collisional system is 3.517 199 6 amu, while the rotational energies of the ion have been computed from its experimental rotational parameters: $B = 1.487 501 00$ cm^{-1}, $D = 2.763 04 \times 10^{-6}$ cm^{-1}, and $H = 2.58 \times 10^{-12}$ cm^{-1} (Ref. 38). Rotational states of HCO^+ with j in the 0–19 range have been included in the calculation and the resulting coupled equations have been solved using a log-derivative propagator with R varying from 2 to 6 Å and in an energy range between 0 and -300 cm^{-1}.

Table II gathers the computed energy differences between the low-lying bound states with negative parity. These values correspond to the rotational transitions of the He–HCO^+ van der Waals complex measured by Salomon *et al.*[24] using double resonance spectroscopy in the ion trap apparatus, which are also reported in Table II. The computed transitions have been fitted by expressing the level energies using the linear rotor expressions as

$$E_J = BJ(J + 1) - DJ^2(J + 1)^2 + HJ^3(J + 1)^3 + LJ^4(J + 1)^4, \quad (9)$$

with B being the rotational constant of the complex and D being the quartic, H being the sextic, and L being the octic centrifugal distortion coefficients. Experimental and theoretical results compare quite well: the average percentage error between individual rotational frequencies is ~0.1%, and the centrifugal trend of the rotational energy is also well reproduced as demonstrated by the fair agreement for the quartic centrifugal distortion constants (~1%) and also for the very small sextic centrifugal distortion constants (~30%, i.e., they agree withing 5σ).

TABLE II. Rotational transitions (MHz) of the He–HCO$^+$ van der Waals complex for $\nu_1 = 0$. Numbers in parentheses are 1σ errors in units of the last quoted digit.

$J'' \leftarrow J'$		Computed[a]	Experimental[b]	% Error
1	0	17 381.457 07	17 395.111 2	0.08
2	1	34 755.089 55	34 782.593 0	0.08
3	2	52 104.049 12	52 154.893 0	0.10
4	3	69 454.387 73	69 504.548 1	0.07
5	4	86 754.361 21	86 824.316 4	0.08
6	5	104 023.156 3	104 107.092 2	0.08
7	6	121 235.500 4	121 345.963 3	0.09
8	7	138 402.605 9	138 534.114 2	0.09
9	8	155 532.417 1	155 664.827 4	0.09
10	9	172 563.476 8	172 731.355 9	0.10
11	10	189 540.723 7	189 726.847 5	0.10
12	11	206 444.761 3	206 644.311 7	0.10
13	12	223 231.250 2	223 476.489 2	0.11
14	13	239 966.924 4	240 215.755 9	0.10
15	14	256 559.927 3	256 853.971 4	0.11
16	15	273 065.801 5	273 382.487 9	0.12
B		8 691.18(59)	8 698.1947(16)	0.08
D		0.322 1(79)	0.318 741(46)	1.07
$H \times 10^5$		6.7(41)	10.03(6)	33.00
$L \times 10^7$		−0.92(70)	−2.681(39)	65.67

[a] Obtained by bound state calculations.
[b] From Ref. 24. Constants of higher order than L are not reported.

IV. SCATTERING CALCULATIONS

A. Inelastic cross sections

Having validated the well depth, the focus of this paper is to provide a new evaluation of the scattering quantities of the HCO$^+$ and He system. We thus solved the standard time-independent coupled scattering equations using the MOLSCAT program.[37] Calculations were carried out at values of the kinetic energy ranging from 2 to 500 cm^{-1} with narrow steps at low energies (0.2 cm^{-1} up to 50 cm^{-1} and 0.5 cm^{-1} up to 170 cm^{-1}), gradually increasing to 5 cm^{-1} up to 500 cm^{-1}). The propagation started at a minimum distance around 2 Å (i.e., where the repulsion barrier of the collisional system is located), whereas the long range limits have been chosen to ensure convergence of the inelastic cross sections over a given energy range. The adopted type of propagator is the hybrid LDMD/AIRY.[39,40] This hybrid approach combines the Manolopoulos diabatic modified log-derivative (LDMD) propagator,[41] operating at short range where the relevant variation in the potential requires strict steps for the propagation, and the Alexander–Manolopoulos Airy (AIRY) propagator[40] at long range, which accounts for looser propagation steps. Such choice provides the best compromise between accuracy and computational efficiency. The rotational basis set has been adjusted in selected energy ranges to ensure convergence of the inelastic cross sections. At the highest total energy considered in the present calculation (500 cm^{-1}), the rotational basis was extended to $j = 32$. The maximum value of the total angular momentum $J = j + l$ used in the
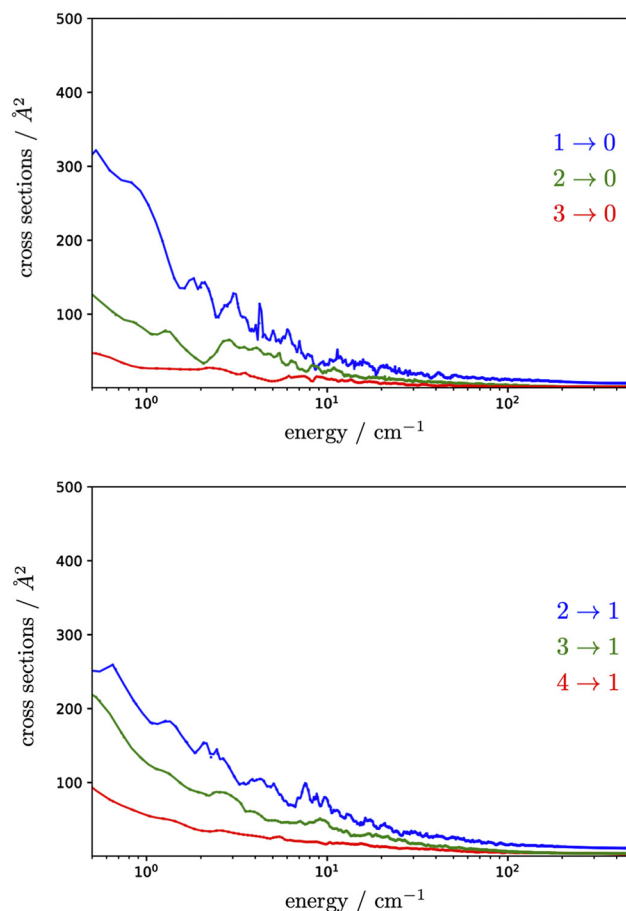
FIG. 3. Trends of some rotational de-excitation cross sections with collisional energy.

calculations was chosen to allow for the convergence of the inelastic cross sections within 0.005 Å^2.

Figure 3 illustrates the energy dependence of the collisional de-excitation cross section for a few selected rotational transitions.

TABLE III. Transition rates for the excitation from j' to j'' at 10 K. Units are 10^{-10} cm^3 s^{-1}.

$j' \rightarrow j''$	This work	Reference 23	Reference 19
$0 \rightarrow 1$	2.322	2.200	1.984
$0 \rightarrow 2$	0.866	0.857	0.739
$0 \rightarrow 3$	0.149	0.143	0.137
$0 \rightarrow 4$	0.022	0.021	0.014
$1 \rightarrow 2$	1.162	1.152	1.099
$1 \rightarrow 3$	0.275	0.266	0.195
$1 \rightarrow 4$	0.030	0.032	0.025
$2 \rightarrow 3$	0.643	0.657	0.566
$2 \rightarrow 4$	0.104	0.097	0.084
$3 \rightarrow 4$	0.390	0.405	0.310

As expected, they show a general decrease as the collisional energy of the system increases. In Fig. 3, the portion up to 500 cm^{-1} has been depicted, where oscillations due to different resonances are discernible for all the selected transitions. This trend is the same as that identified by Yazidi et al.[42] for the HCO$^+$ and H$_2$ collisional system and is due to the presence of a potential well that supports many bound states.

B. State-to-state transition rates

The collisional calculations provide a set of inelastic cross sections as a function of the collision energy $\sigma(E_c)$. Starting from these quantities, we have obtained the corresponding excitation and de-excitation rate coefficients, $k_{j' \rightarrow j''}(T)$ for temperatures ranging from 5 to 100 K. This was accomplished by averaging the $\sigma(E_c)$ over the collision energy,

$$k_{j' \rightarrow j''}(T) = \left(\frac{8}{\pi \mu k^3 T^3} \right)^{1/2} \int_0^\infty \sigma_{j' \rightarrow j''}(E_c) E_c \exp(-E_c/kT) dE_c, \tag{10}$$

where k is the Boltzmann constant and μ is the reduced mass of the system. Some excitation rate coefficients are listed in Table III, thus enabling a comparison with those calculated in two previous studies.[19,23] The agreement is good, especially when compared with the most recent results,[23] with an absolute maximum deviation of only 0.1×10^{-10} cm^3 s^{-1}. Figure 4 illustrates the temperature dependence of some de-excitation coefficients up to 100 K and the rate
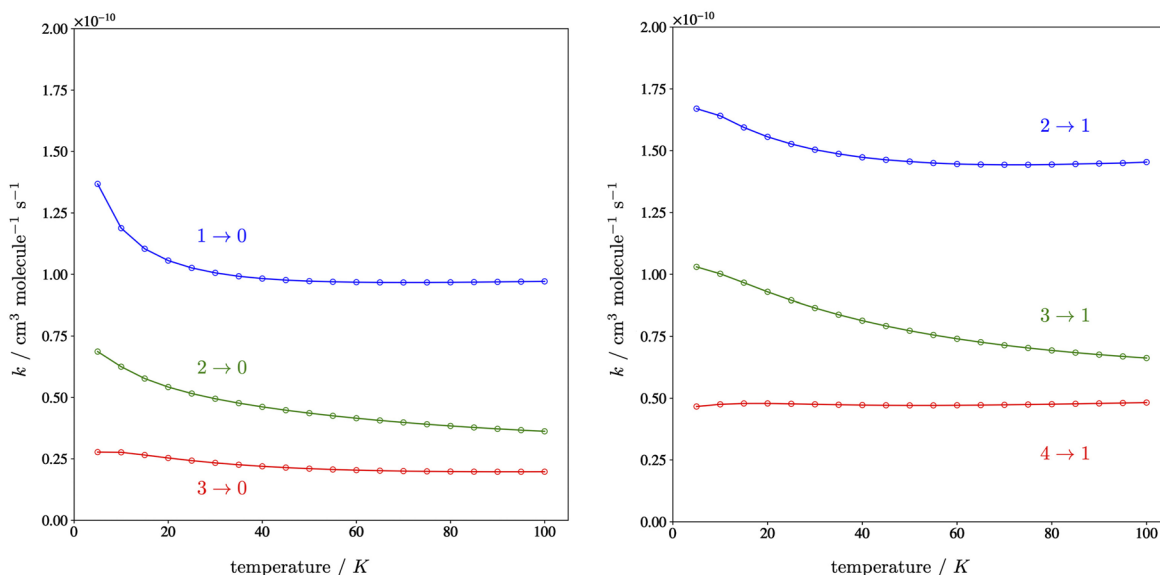

FIG. 4. Variation with temperature of some rotational de-excitation rate coefficients.
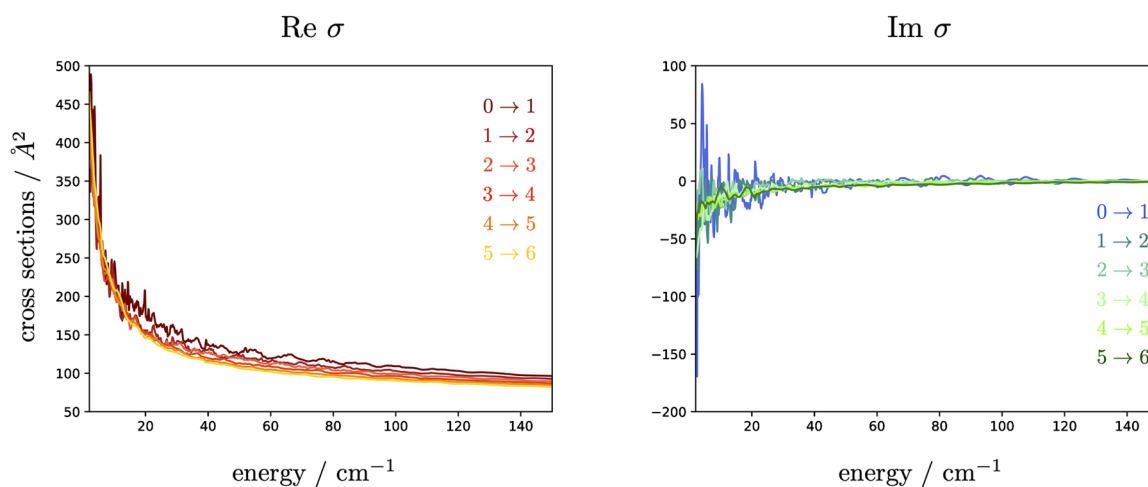

FIG. 5. Dependence of σ on the thermal energy of the system for the six lowest rotational transitions.

TABLE IV. Computed broadening cross section obtained by integration over the thermal energy distribution for the HCO$^+$ and He system at 88 K.

$j'' \leftarrow j'$	This work (Å^2)		Reference 20 (Å^2)	
	Re σ	Im σ	Re σ	Im σ
$1 \leftarrow 0$	113.120	1.354	110.05	1.23
$2 \leftarrow 1$	106.850	1.205	104.06	1.33
$3 \leftarrow 2$	104.158	1.056	101.04	1.12
$4 \leftarrow 3$	101.160	1.622	98.19	1.83
$5 \leftarrow 4$	98.507	2.378	95.66	2.51
$6 \leftarrow 5$	96.459	2.701	93.79	2.89

coefficients for the transitions $(1, 2, 3) \rightarrow 0$ and $(2, 3, 4) \rightarrow 1$. One can clearly see that at low temperatures, the rate coefficients tend to decrease by increasing the energy. This trend significantly fades as Δj increases, becoming hardly discernible for $\Delta j = 3$. At higher temperature, all the rate coefficients become almost independent of the temperature, thus reflecting the prediction of the Langevin theory for ion–neutral interactions. A comprehensive list of the integrated de-excitation rate coefficients up to $j = 5$ is presented in Tables I and II of the supplementary material.

C. Pressure broadening and shift

The pressure broadening and pressure shift coefficients were evaluated for the six lowest-energy rotational transitions for which Buffa *et al.* computed results and some experimental counterparts[20] are also available.

For this purpose, the S-matrices obtained from scattering calculations have been employed. The computation of these cross sections requires S-matrix elements involving both the initial and final states of the examined transition, which have the same kinetic energy but different total energies. The real (Re) and imaginary (Im) parts of the cross sections for a pair of upper and lower states describe the pressure broadening and shift, respectively, of a given $j'' \leftarrow j'$ line.

The trend of the cross sections over the energy distribution shows irregular oscillations for all the studied transitions. This behavior is discernible from Fig. 5, where the oscillations are clearly visible in the lower energy portion and are particularly pronounced for the transitions involving the low lying states. The final cross sections were calculated by integrating over the entire distribution of the thermal energy,

$$\bar{\sigma} = \frac{1}{(kT)^2} \int_0^\infty E e^{-E/kT} \sigma(E) dE, \qquad (11)$$

where k is the Boltzmann constant and T is the temperature chosen for the integration, which was set to 88 K to allow for the comparison with previously calculated and observed values. The resulting pressure broadening cross sections are collected in Table IV, where the previous results by Buffa *et al.*[20] are also reported.

The associated pressure broadening (Γ) and pressure shift (s) coefficients are obtained from the real and imaginary parts of the cross sections, respectively, as

$$\Gamma - \mathrm{i}s = n_p \bar{v} \bar{\sigma} = \frac{56.691\,5}{\sqrt{\mu T}} \bar{\sigma}, \qquad (12)$$

$\bar{v} = (8k_B T / \pi \mu)^{1/2}$ is the mean velocity of the colliders and n_p represents the density of the gas. In terms of units, Γ and s are expressed in cm^{-3} atm^{-1}, $\bar{\sigma}$ in A^2, μ (reduced mass of the system) in amu, and T in kelvin.

The resulting coefficients are listed in Table V, where the comparison with the experimental and previously computed counterparts is also reported. A first noteworthy point is a discrepancy observed between the coefficients presented in Ref. 20 and the coefficients recalculated from the cross sections obtained by the same paper via Eq. (12). Both values have been reported in the last two columns of Table V. This discrepancy may be attributable to an error in the cross section conversion since a systematic shift is observed for

TABLE V. Measured and calculated pressure broadening and shift parameters for the HCO$^+$ and He system at 88 K.

$j'' \leftarrow j'$	Frequency (MHz)	Parameter	Exp. values (MHz/Torr)	This work (MHz/Torr)	Recomputed values[a] (MHz/Torr)	Reference 20 (MHz/Torr)
$1 \leftarrow 0$	89 188.5261	Broadening		14.377	13.987	13.76
		Shift		0.172	0.156	0.154
$2 \leftarrow 1$	178 375.0642	Broadening		13.580	13.225	13.01
		Shift		0.153	0.169	0.168
$3 \leftarrow 2$	267 557.6263	Broadening		13.238	12.841	12.64
		Shift		0.134	0.142	0.134
$4 \leftarrow 3$	356 734.2246	Broadening	12.39(29)	12.857	12.479	12.27
		Shift	0.328(19)	0.206	0.233	0.229
$5 \leftarrow 4$	445 902.8713	Broadening	12.42(22)	12.520	12.158	11.95
		Shift	0.427(29)	0.302	0.319	0.312
$6 \leftarrow 5$	535 061.5791	Broadening	12.13(29)	12.260	11.920	11.72
		Shift	0.497(17)	0.343	0.367	0.364

[a]Recomputed values from the cross sections taken from Table 2 of Ref. 20.

almost all transitions. Indeed, by reconverting the cross sections at 91 K instead of 88 K, our results became very close to those reported by Buffa et al.[20]

The comparison of the computed data with those experimentally measured revealed a remarkable agreement. It appears that the PES computed in this work describes more accurately the pressure-broadening parameters related to the two higher energy transitions, where the percentage error with respect to the experiments is around 1%. A somewhat larger discrepancy is exhibited by the $4 \leftarrow 3$ transition for which the percentage error is ~4%. On the other hand, pressure shift coefficients, derived from the imaginary part of the broadening cross sections, show larger deviations compared to experiments. It should be noted, however, that such measurements are rather delicate and thus affected by significant uncertainties. Nevertheless, from a qualitative point of view, their values show a good agreement with those computed in this work.

V. CONCLUSIONS

In this work, the evaluation and validation of an accurate computational procedure for the characterization of collisional potential energy surfaces has been reported. This investigation drew on the excellent performance of explicitly correlated methods for the description of both short- and long-range interaction energies, whose affordable computational cost would also allow a straightforward extension of this methodology to larger collisional systems.

The chosen molecular system (HCO^+ and He) provided an excellent test case for the study of long-range effects and led to a complete derivation of all the relevant scattering parameters at the best accuracy achieved so far.

The validation of the resulting data with the experimental counterparts and the computational results from previous works led to a further proof of the accuracy of the computational procedure. For instance, the comparison of the rotational frequencies of the bound state obtained by means of a pure computational methodology with the corresponding experimental values revealed a percentage error always smaller than 0.12%. Furthermore, the obtained pressure coefficients are in good agreement with the previously experimentally measured values over three rotational transitions. However, a more thorough analysis of our computational performance would be more significant if a greater number of experimental transitions were accessible.

SUPPLEMENTARY MATERIAL

See the supplementary material for the complete list of the computed de-excitation rate coefficients from 5 to 100 K.

AUTHOR DECLARATIONS

Conflict of Interest

The authors have no conflicts to disclose.

DATA AVAILABILITY

The data that support the findings of this study are available within the article and its supplementary material.

REFERENCES

[1] E. Roueff and F. Lique, "Molecular excitation in the interstellar medium: Recent advances in collisional, radiative, and chemical processes," Chem. Rev. **113**(12), 8906–8938 (2013).

[2] J. Kauffmann, P. F. Goldsmith, G. Melnick, V. Tolls, A. Guzman, and K. M. Menten, "Molecular line emission as a tool for galaxy observations (LEGO). I. HCN as a tracer of moderate gas densities in molecular clouds and galaxies," Astron. Astrophys. **605**, L5 (2017).

[3] T. B. Adler, G. Knizia, and H.-J. Werner, "A simple and efficient CCSD(T)-F12 approximation," J. Chem. Phys. **127**, 221106 (2007).

[4] G. Knizia, T. B. Adler, and H.-J. Werner, "Simplified CCSD(T)-F12 methods: Theory and benchmarks," J. Chem. Phys. **130**(5), 054104 (2009).

[5] K. A. Peterson, T. B. Adler, and H.-J. Werner, "Systematically convergent basis sets for explicitly correlated wavefunctions: The atoms H, He, B–Ne, and Al–Ar," J. Chem. Phys. **128**(8), 084102 (2008).

[6] R. A. Kendall, T. H. Dunning, Jr., and R. J. Harrison, "Electron affinities of the first-row atoms revisited. Systematic basis sets and wave functions," J. Chem. Phys. **96**(9), 6796–6806 (1992).

[7] F. Lique, J. Kłos, and M. Hochlaf, "Benchmarks for the generation of interaction potentials for scattering calculations: Applications to rotationally inelastic collisions of C_4 ($X^3\Sigma_g^-$) with He," Phys. Chem. Chem. Phys. **12**(48), 15672–15680 (2010).

[8] Y. Ajili, K. Hammami, N. E. Jaidane, M. Lanza, Y. N. Kalugina, F. Lique, and M. Hochlaf, "On the accuracy of explicitly correlated methods to generate potential energy surfaces for scattering calculations and clustering: Application to the HCl–He complex," Phys. Chem. Chem. Phys. **15**(25), 10062–10070 (2013).

[9] S. Petrie and D. K. Bohme, "Ions in space," Mass Spectrom. Rev. **26**(2), 258–280 (2007).

[10] E. Herbst, "Molecular ions in interstellar reaction networks," J. Phys.: Conf. Ser. **4**, 17 (2005).

[11] L. E. Snyder, J. M. Hollis, F. J. Lovas, and B. L. Ulich, "Detection, identification, and observations of interstellar $H^{13}CO^+$," Astrophys. J. **209**, 67–74 (1976).

[12] W. D. Langer, R. W. Wilson, P. S. Henry, and M. Guelin, "Observations of anomalous intensities in the lines of the HCO^+ isotopes," Astrophys. J. **225**, L139–L142 (1978).

[13] W. J. Welch, M. C. H. Wright, R. L. Plambeck, J. H. Bieging, and B. Baud, "Millimeter-wavelength aperture synthesis of molecular lines toward Orion KL," Astrophys. J. **245**, L87–L90 (1981).

[14] V. Lattanzi, A. Walters, B. J. Drouin, and J. C. Pearson, "Rotational spectrum of the formyl cation, HCO^+, to 1.2 THz," Astrophys. J. **662**(1), 771 (2007).

[15] P. Caselli, C. M. Walmsley, R. Terzieva, and E. Herbst, "The ionization fraction in dense cloud cores," Astrophys. J. **499**(1), 234 (1998).

[16] D. Buhl and L. E. Snyder, "Unidentified interstellar microwave line," Nature **228**(5268), 267–269 (1970).

[17] R. C. Woods, T. A. Dixon, R. J. Saykally, and P. G. Szanto, "Laboratory microwave spectrum of HCO^+," Phys. Rev. Lett. **35**, 1269–1272 (1975).

[18] O. Denis-Alpizar, T. Stoecklin, A. Dutrey, and S. Guilloteau, "Rotational relaxation of HCO^+ and DCO^+ by collision with H_2," Mon. Not. R. Astron. Soc. **497**(4), 4276–4281 (2020).

[19] T. S. Monteiro, "Rotational excitation of HCO^+ by collisions with H_2," Mon. Not. R. Astron. Soc. **214**(4), 419–427 (1985).

[20] G. Buffa, L. Dore, F. Tinti, and M. Meuwly, "Experimental and theoretical study of helium broadening and shift of HCO^+ rotational lines," ChemPhysChem **9**(15), 2237–2244 (2008).

[21] K. Raghavachari, G. W. Trucks, J. A. Pople, and M. Head-Gordon, "A fifth-order perturbation comparison of electron correlation theories," Chem. Phys. Lett. **157**(6), 479–483 (1989).

[22] K. A. Peterson, D. E. Woon, and T. H. Dunning, Jr., "Benchmark calculations with correlated molecular wave functions. IV. The classical barrier height of the $H + H_2 \rightarrow H_2 + H$ reaction," J. Chem. Phys. **100**(10), 7410–7415 (1994).

[23] G. Buffa, L. Dore, and M. Meuwly, "State-to-state rotational transition rates of the HCO^+ ion by collisions with helium," Mon. Not. R. Astron. Soc. **397**(4), 1909–1914 (2009).

[24] T. Salomon, M. Töpfer, P. Schreier, S. Schlemmer, H. Kohguchi, L. Surin, and O. Asvany, "Double resonance rotational spectroscopy of $He–HCO^+$," Phys. Chem. Chem. Phys. **21**, 3440–3445 (2019).

[25] P. B. Davies and W. J. Rothwell, "Diode laser detection of the bending mode of HCO^+," J. Chem. Phys. **81**(12), 5239–5240 (1984).

[26] L. Dore, S. Beninati, C. Puzzarini, and G. Cazzoli, "Study of vibrational interactions in DCO^+ by millimeter-wave spectroscopy and determination of the equilibrium structure of the formyl ion," J. Chem. Phys. **118**, 7857–7862 (2003).

[27] T. H. Dunning, Jr., "Gaussian basis sets for use in correlated molecular calculations. I. The atoms boron through neon and hydrogen," J. Chem. Phys. **90**(2), 1007–1023 (1989).

[28] D. E. Woon and T. H. Dunning, Jr., "Gaussian basis sets for use in correlated molecular calculations. III. The atoms aluminum through argon," J. Chem. Phys. **98**(2), 1358–1371 (1993).

[29] E. Papajak, J. Zheng, X. Xu, H. R. Leverentz, and D. G. Truhlar, "Perspectives on basis sets beautiful: Seasonal plantings of diffuse basis functions," J. Chem. Theory Comput. **7**(10), 3027–3034 (2011).

[30] S. Alessandrini, V. Barone, and C. Puzzarini, "Extension of the 'cheap' composite approach to noncovalent interactions: The jun-ChS scheme," J. Chem. Theory Comput. **16**(2), 988–1006 (2019).

[31] J. D. Watts, J. Gauss, and R. J. Bartlett, "Coupled-cluster methods with noniterative triple excitations for restricted open-shell Hartree–Fock and other general single determinant reference functions. Energies and analytical gradients," J. Chem. Phys. **98**(11), 8718–8733 (1993).

[32] H.-J. Werner, P. J. Knowles, G. Knizia, F. R. Manby, and M. Schütz, "Molpro: A general-purpose quantum chemistry program package," Wiley Interdiscip. Rev.: Comput. Mol. Sci. **2**, 242–253 (2012).

[33] D. Feller, "Application of systematic sequences of wave functions to the water dimer," J. Chem. Phys. **96**(8), 6104–6114 (1992).

[34] T. Helgaker, W. Klopper, H. Koch, and J. Noga, "Basis-set convergence of correlated calculations on water," J. Chem. Phys. **106**(23), 9639–9646 (1997).

[35] S. F. Boys and F. Bernardi, "The calculation of small molecular interactions by the differences of separate total energies. Some procedures with reduced errors," Mol. Phys. **19**(4), 553–566 (1970).

[36] F. Lique and A. Faure, *Gas-Phase Chemistry in Space; From Elementary Particles to Complex Organic Molecules* (IOP Astronomy, 2019).

[37] J. M. Hutson and C. Sueur, "User manual for MOLSCAT, BOUND and FIELD, version 2020.0: Programs for quantum scattering properties and bound states of interacting pairs of atoms and molecules," arXiv:1903.06755 (2019).

[38] G. Cazzoli, L. Cludi, G. Buffa, and C. Puzzarini, "Precise THz measurements of HCO^+, N_2H^+, and CF^+ for astrophysical observations," Astrophys. J., Suppl. Ser. **203**, 11 (2012).

[39] M. H. Alexander, "Hybrid quantum scattering algorithms for long-range potentials," J. Chem. Phys. **81**(10), 4510–4516 (1984).

[40] M. H. Alexander and D. E. Manolopoulos, "A stable linear reference potential algorithm for solution of the quantum close-coupled equations in molecular scattering theory," J. Chem. Phys. **86**(4), 2044–2050 (1987).

[41] D. E. Manolopoulos, "An improved log derivative method for inelastic scattering," J. Chem. Phys. **85**(11), 6425–6429 (1986).

[42] O. Yazidi, D. Ben Abdallah, and F. Lique, "Revised study of the collisional excitation of HCO^+ by H_2 (j = 0)," Mon. Not. R. Astron. Soc. **441**(1), 664–670 (2014).

24 January 2024 14:39:16